CSIRO PUBLISHING

Australian Journal of Physics

Volume 52, 1999

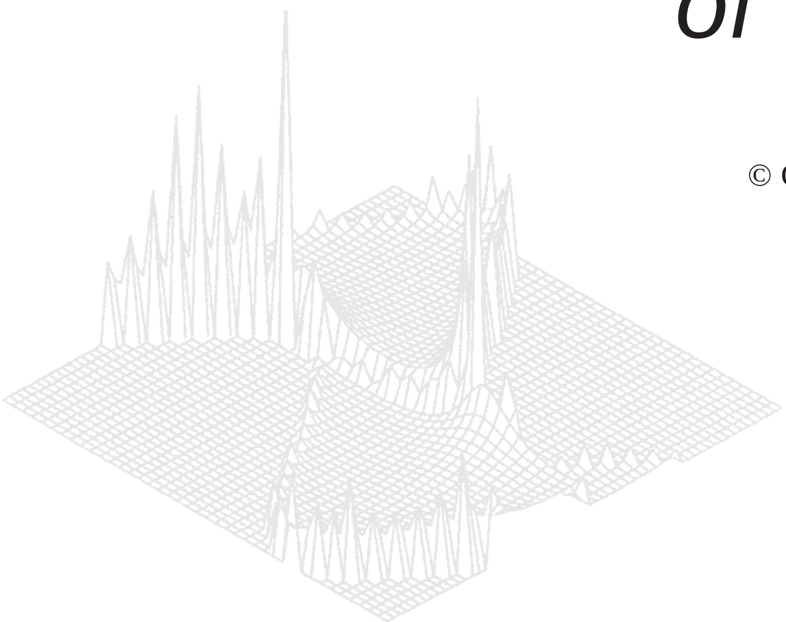

A journal for the publication of
original research in all branches of physics

www.publish.csiro.au/journals/ajp

All enquiries and manuscripts should be directed to
Australian Journal of Physics
CSIRO PUBLISHING
PO Box 1139 (150 Oxford St)
Collingwood
Vic. 3066
Australia
Telephone: 61 3 9662 7626
Facsimile: 61 3 9662 7611
Email: peter.robertson@publish.csiro.au

Published by **CSIRO** PUBLISHING
for CSIRO Australia and
the Australian Academy of Science

Aust. J. Phys., 1999, **52**, 697–714

Quadratic Solitons: New Possibility for All-optical Switching*

A. V. Buryak and V. V. Steblina

School of Mathematics and Statistics, Australian Defence Force Academy,
Canberra, ACT 2600, Australia.
Optical Sciences Centre, Research School of Physical Sciences and Engineering,
Australian National University, Canberra, ACT 0200, Australia.

Abstract

We discuss potential applications of quadratic optical solitons for all-optical switching in bulk quadratic nonlinear media. Among the major phenomena investigated are soliton scattering, spiralling, fusion, and also power exchange between the colliding solitons.

1. General Introduction

> The communications network ... will enable the consciousness of our grandchildren to flicker like lightning back and forth across the face of this planet. They will be able to go anywhere and meet anyone at any time without stirring from their homes. All the museums and libraries of the world will be extensions of their living rooms.
>
> Arthur C. Clarke, Voices from the Sky,
> (Harper & Row, 1965)

The author of *'2001: A Space Odyssey'* would no doubt be pleased that his vision of a world connected by instantaneous communications did arrive as predicted. This leap from vision to reality has been exponential, not gradual. The most sweeping changes in communications over the past three decades have been compressed into the short space of the past few years. Bit by bit, the Earth's surface is being criss-crossed by a network of optical fibres, connecting countries across oceans, and connecting cities across vast distances. In the modern 'information society', large-capacity and reliable local, national and international telecommunications networks pave the way for the convergence of computers, advanced communications, information and entertainment. Before a national *information superhighway* can emerge, the 'roads' must be widened and the 'freight' – text, data, images, voice or video signals – must be digitised, packaged and tagged so that it can be bussed speedily and accurately from end to end.

Modern telecommunications networks rely on the unmatched capacity of silica-based optical fibres to carry information. Currently optical fibre links are

* Refereed paper based on the Bragg Lecture presented by AVB on 28 September 1998 at the 13th AIP National Congress held in Fremantle, Western Australia.

 10.1071/PH98117 0004-9506/99/040697$10.00

replacing traditional copper cabling in the world's infrastructure. Copper coaxial cables are inadequate for transmitting high-volume data, whereas optical fibres have essentially unlimited capacity. In a practical network, the majority of optical fibres are still interconnected by electronic devices, which provide necessary switching and signal processing functions. Therefore, significant limitations on the bit-rate capacity and cost of these hybrid networks are imposed by the speed of electronic processing and the need to convert signals from light to electricity and back to light again. This is one reason why current optical fibre systems utilise only a minute fraction of available capacity.

An ultimate goal for fibre optics is the creation of *all-optical networks* that run entirely in glass. Unlike existing fibre optic networks, which convert light signals to electronic form in order to amplify or switch them, the *all-optical network is entirely photonic*. It will carry information-bearing laser-light pulses in dozens of wavelengths to create tens of thousands of channels that can be switched and guided by simple photonic devices.

Historically, the new era in integrated photonics research started in 1969, when the concept of *integrated optics* was proposed (Miller 1969). Research on optical integrated circuits (OIC), where certain electronic functions were replaced with photonic equivalents, started in the early 1970*s*, when various materials and processing techniques for waveguides were investigated. Through this research, the main features of glass, $LiNbO_3$, polymer and semiconductor waveguides were revealed. Recent developments in optical planar waveguides, especially in the buried channel waveguide (BCW) technology (see e.g. Kawachi 1990) represent a major step towards the super-capacity, super-fast 'transparent' optical fibre networks of the future.

Nowadays the vast majority of optical fibres and passive optical processing elements are used as linear devices (i.e. their characteristics do not depend on the intensity of the incident signal) (Snyder and Love 1983). Linear optical devices are very versatile and cover a broad range of network applications including power splitting, coupling and wavelength multiplexing/demultiplexing of signals. Although they are ideal for some processing duties, linear waveguide devices are, by definition, unsuitable for power switching. The key to developing photonic switches is the discovery of nonlinear optical materials whose refractive index can vary rapidly in response to changing light intensity. Two principal schemes of nonlinear switching devices are shown in Fig. 1. Clearly, an intensity-dependent response is necessary in both of the cases presented.

Initially the optical materials with a cubic nonlinear response (so-called Kerr or $\chi^{(3)}$ materials) were proposed for ultra-high-speed signal processing (see e.g. Stegeman *et al*. 1988). By now many types of nonlinear all-optical devices [e.g. nonlinear optical couplers (Jensen 1982; Friberg *et al*. 1988), nonlinear Mach–Zehnder interferometers (Baek *et al*. 1995) and nonlinear mode-mixers (Wa *et al*. 1988) etc.] have been designed and implemented experimentally. Despite all this progress it has been realised that the overall material properties required for the applications mentioned are very stringent, and to date only a few suitable materials have been identified. Unfortunately, the value of the Kerr-type nonlinearity of conventional (silica-based) optical materials is very small, and this makes it difficult to design and produce highly efficient and compact nonlinear optical devices for use at acceptably low intensities. Among the organic $\chi^{(3)}$ optical materials (polymers) the situation is encouraging, but far from perfect: organic materials with high electronic Kerr nonlinearities are lossy and not environmentally stable. For this reason researchers have not been very optimistic about effective signal processing using Kerr-type nonlinear devices under realistic conditions.

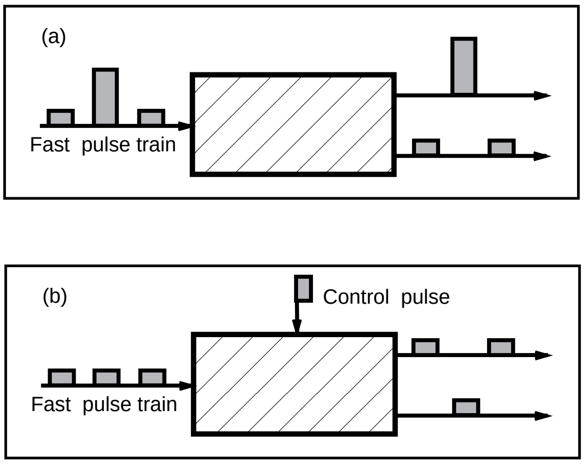

Fig. 1. Two principal schemes for nonlinear switching devices.

However, recent studies of nonlinear wave propagation in a different medium, namely quadratic (or $\chi^{(2)}$) optical materials, have made many researchers more optimistic. The second-order nonlinearity is traditionally associated with second-harmonic generation (SHG; Schubert and Wilhelmi 1986), and was not, until recently, seen as a source of self-guiding and switching phenomena. This view has now changed, and it has been demonstrated (De Salvo *et al.* 1992) that under certain conditions $\chi^{(2)}$ nonlinear materials can behave very similarly to conventional Kerr materials, due to so-called *cascaded* $\chi^{(2)}$ nonlinear effects, producing very high effective nonlinearities. The newly discovered cascading phenomenon is opening up opportunities for novel nonlinear switching schemes.

The active experimental research on cascaded $\chi^{(2)}$ nonlinear effects renewed interest in the fundamental concept of *guiding light by light itself*, which had been suggested and developed in the 1980s (see e.g. Azimov *et al.* 1987; Shen *et al.* 1988). This concept takes advantage of *spatial solitons*, which are self-guiding optical beams existing due to the balance between diffraction and nonlinearity. Stable spatial solitons open up exciting prospects of creating *reconfigurable guiding structures* in nonlinear optical materials. Spatial solitons have attracted substantial research interest because of their potential applications in all-optical switching (see e.g. Segev and Stegeman 1998). In general it is well known that (1+1)-dimensional solitons [see Fig. 2, which presents the schematics of (1+1)- and (2+1)-dimensional solitons] are expected to interact (attract, repel, etc.) as effective particles (Gorshkov and Ostrovsky 1981; Karpman and Solov'ev 1981). However, the most promising schemes for all-optical switching can be based on *non-planar* soliton collisions and steering in a bulk medium (Steblina *et al.* 1998), where full advantage can be taken of the three-dimensional geometry.

Although (2+1)-dimensional solitons of a pure Kerr medium are unstable and cannot be employed for soliton switching, recent experimental discoveries of *stable (2+1)-dimensional solitons* in different nonlinear media (Torruellas *et al*. 1995; Duree *et al*. 1993; Tikhonenko *et al*. 1995) have renewed interest in three-dimensional interactions between solitary beams.

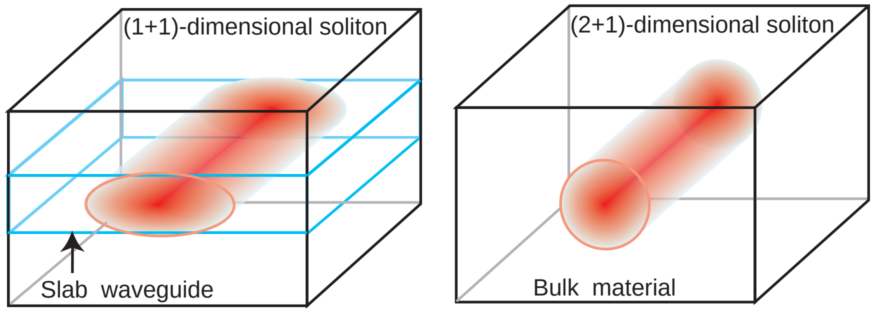

Fig. 2. Qualitative pictures of (1+1)- and (2+1)-dimensional spatial solitons.

Among other types of spatial self-guiding beams, $\chi^{(2)}$ solitons are especially attractive for all-optical switching, because the nonlinear response of quadratic media occurs on an ultra-fast time scale of femtoseconds (see e.g. the recent review by Stegeman *et al*. 1996). Head-on (planar) collisions of (2+1)-dimensional $\chi^{(2)}$ solitons have previously been investigated numerically (Buryak *et al*. 1995; Leo *et al*. 1997*a*, 1997*b*); it was shown that soliton collisions depend strongly on the initial relative phase between the beams, similar to the case of one-wave non-Kerr solitons described by the generalised nonlinear Schrödinger equation. When the relative phase between the two colliding solitons is zero, they attract each other and finally fuse into a single soliton of a larger amplitude. The amplitude of this 'fused' soliton oscillates due to the excitation of a soliton internal mode (Etrich *et al*. 1996). However, when the two interacting solitons are significantly out of phase, the interaction between them can be repulsive, and both solitons, after exchanging some energy, survive after the collision. Switching in slab $\chi^{(2)}$ waveguides and bulk crystals based on head-on soliton collisions has been recently observed experimentally (Baek *et al*. 1997; Costantini *et al*. 1998). Non-planar collisions of $\chi^{(2)}$ solitons have not been addressed previously, except our earlier Letter (Steblina *et al*. 1998).

In spite of all this recent progress, no systematic theory of non-planar soliton interactions in a bulk medium has been developed so far. In the majority of previous investigations, the theoretical analysis has been limited to direct numerical simulations only, which, on their own, usually fail to give *general* predictions or conclusions. In this paper we generalise the effective particle approach (EPA) of Gorshkov and Ostrovsky (1981) to describe non-planar collisions of optical beams in a bulk nonlinear medium, taking the case of (2+1)-dimensional $\chi^{(2)}$ solitons as an important and practical example. We demonstrate several regimes of non-planar soliton collisions, including scattering, spiralling, fusion and power exchange. Our model allows significant simplification of the analysis of beam interactions, and also provides an important physical insight. On the other hand, very good agreement is achieved with the results obtained by direct numerical modelling.

2. Model Formulation and Summary of Stability Results

We consider beam propagation in lossless $\chi^{(2)}$ nonlinear media under appropriate conditions for type I SHG (two-wave parametric mixing). In *esu*, the system of equations that describes the interaction of the first fundamental ($\omega_1 = \omega$) and second ($\omega_2 = 2\omega$) harmonics in a *weakly* anisotropic medium with $\chi^{(2)}$ nonlinear susceptibility has the following form [see Menyuk and Torner (1994) for details of the derivation]:

$$
\begin{aligned}
&2ik_1 \frac{\partial E_1}{\partial \tilde{z}} + \nabla_\perp^2 E_1 + \frac{8\pi\omega_1^2}{c^2}\chi^{(2)} E_2 E_1^* e^{-i\delta k \tilde{z}} = 0, \\
&2ik_2 \frac{\partial E_2}{\partial \tilde{z}} + \nabla_\perp^2 E_2 + \frac{16\pi\omega_1^2}{c^2}\chi^{(2)} E_1^2 e^{i\delta k \tilde{z}} = 0,
\end{aligned}
\tag{1}
$$

where E_1 and E_2 are the complex scalar electric field amplitude envelopes, the asterisk denotes complex conjugation, $\nabla_\perp^2 = \partial^2/\partial\tilde{x}^2$ for the (1+1)-dimensional case of slab waveguide geometry, or $\nabla_\perp^2 = \partial^2/\partial\tilde{x}^2 + \partial^2/\partial\tilde{y}^2$ for (2+1)-dimensional bulk media; $\delta k \equiv (2k_1 - k_2) \equiv 2[n(\omega) - n(2\omega)]\omega/c$ is the wavevector mismatch between the first and second harmonics, n is the linear refractive index of the medium; $\tilde{z}$ is the longitudinal coordinate parallel to the direction of propagation, $\tilde{x}$ and $\tilde{y}$ are the transverse coordinates, and the $\chi^{(2)}$ coefficient is proportional to the relevant element of the corresponding nonlinear susceptibility tensor. Note that the system (1) is only valid when the spatial walk-off is negligible, although this can also be taken into account (see e.g. Menyuk and Torner 1994; Buryak and Kivshar 1995).

Normalising the transverse coordinates in terms of the beam radius R_0 (it can be defined in various ways, e.g. as the half-width at the $1/e$ intensity point), then $\tilde{x} = R_0 x$, $\tilde{y} = R_0 y$. The longitudinal coordinate is normalised as $\tilde{z} = R_d z$, i.e. in units of the diffraction length $R_d \equiv 2R_0^2 k_1$. If we define R_0 as the half-width at the $1/e$ intensity point, then a Gaussian-shaped beam $|E_1|^2 \sim \exp[-(\tilde{x}^2 + \tilde{y}^2)/R_0^2]$ will spread as $R_0^2(\tilde{z}) = R_0^2(0)[1 + (2\tilde{z}/R_d)^2]$ in a linear isotropic medium. Finally, the fields E_1 and E_2 are normalised according to

$$
\begin{aligned}
E_1 &= \frac{vc^2}{16\pi\omega_1^2\chi^{(2)}R_0^2}, \\
E_2 &= \frac{wc^2}{8\pi\omega_1^2\chi^{(2)}R_0^2}\, e^{i\delta k R_d z},
\end{aligned}
\tag{2}
$$

to get the normalised system

$$
\begin{aligned}
&i\frac{\partial v}{\partial z} + \frac{\partial^2 v}{\partial x^2} + \frac{\partial^2 v}{\partial y^2} + wv^* = 0, \\
&i\sigma\frac{\partial w}{\partial z} + \frac{\partial^2 w}{\partial x^2} + \frac{\partial^2 w}{\partial y^2} - \sigma\Delta w + \frac{v^2}{2} = 0,
\end{aligned}
\tag{3}
$$

where $\Delta \equiv R_d \delta k$ is the dimensionless mismatch parameter, and $\sigma \equiv k_2/k_1 = 2\cdot 0$ for the case of spatial solitons. We will call σ and Δ the *system* parameters. These parameters are fixed by the experimental setup. We note that we use equations (3), rather than other forms of normalised equations [e.g. the form used by Buryak *et al*. (1995)], because the former system leads to much simpler equations for soliton interaction.

Although the system (3) is not integrable analytically, it possesses several integrals of motion. Among these integrals, the Manley–Rowe (power) invariant is especially important for our analysis:

$$Q = \int_{-\infty}^{\infty}\int_{-\infty}^{\infty} \left(|v|^2 + 2\sigma|w|^2\right) dx\, dy\,. \tag{4}$$

There are also two momentum-type invariants and a Hamiltonian invariant.

The number of integrals of motion of the evolution system is closely related to the number of internal parameters of the respective soliton families (Gorshkov and Ostrovsky 1981). Usually each of the energy- and momentum-type invariants corresponds to the existence of one internal soliton parameter. In this instance we can expect equations (3) to have a three-parameter bright soliton family. In order to find this three-parameter family explicitly, we represent the v and w components as

$$\begin{aligned} v(x,y,z) &= V(x - C_x z, y - C_y z, z)e^{i\beta z},\\ w(x,y,z) &= W(x - C_x z, y - C_y z, z)e^{2i\beta z}, \end{aligned} \tag{5}$$

and then find (e.g. numerically) complex *stationary*, i.e. z-independent, localised solutions of the system

$$\begin{gathered} \frac{\partial^2 V}{\partial x^2} + \frac{\partial^2 V}{\partial y^2} - iC_x\frac{\partial V}{\partial x} - iC_y\frac{\partial V}{\partial y} - \beta V + WV^* = 0,\\ \frac{\partial^2 W}{\partial x^2} + \frac{\partial^2 W}{\partial y^2} - i\sigma C_x\frac{\partial W}{\partial x} - i\sigma C_y\frac{\partial W}{\partial y} - \sigma(2\beta+\Delta)W + \frac{V^2}{2} = 0\,. \end{gathered} \tag{6}$$

In equations (6) we have introduced the real *internal* soliton parameters β, C_x and C_y, which, in contrast to the *system* parameters σ and Δ, may change during soliton evolution and interactions. The soliton parameter β is the nonlinearly-induced shift of the propagation constant, whereas C_x and C_y are two components of the soliton velocity.

For fixed σ and Δ, complex stationary soliton solutions of equations (6) are defined by values of the *internal* soliton parameters β, C_x and C_y, and can be written down as $V_s(\beta, C_x, C_y; x, y)$, $W_s(\beta, C_x, C_y; x, y)$. If all possible zero-velocity stationary solitons $V_s(\beta, 0, 0; x, y)$, $W_s(\beta, 0, 0; x, y)$ are known [such soliton solutions have been found both numerically and semi-analytically (Buryak *et al*. 1995; Steblina *et al*. 1995)] then for $\sigma = 2$ we can find non-zero velocity solitons of equations (6) using the well-known gauge invariance property (Buryak *et al.* 1995). Indeed, by direct substitution, one can show that

$$V_s(\beta, C_x, C_y; x, y) = V_s\Big(\beta - \frac{C_x^2}{4} - \frac{C_y^2}{4}, 0, 0; x, y\Big) e^{i(C_x x + C_y y)/2},$$

$$W_s(\beta, C_x, C_y; x, y) = W_s\Big(\beta - \frac{C_x^2}{4} - \frac{C_y^2}{4}, 0, 0; x, y\Big) e^{i(C_x x + C_y y)}. \tag{7}$$

The 'moving' solitons given by equations (7) can be used as initial conditions in numerical analysis of soliton collisions.

The full-scale theoretical analysis of the existence and stability of single bright solitons described by equations (3) is beyond the scope of this work. However, for completeness of the presentation, we present major results below. Detailed analysis of this and similar problems can be found in Buryak *et al.* (1995, 1996) and Pelinovsky *et al.* (1995).

It is possible to show that the domain of soliton existence is given by

$$\left(\beta - \frac{C_x^2}{4} - \frac{C_y^2}{4}\right) > \max\left(0, -\frac{\Delta}{2}\right). \tag{8}$$

Using an analysis similar to that reported by Buryak *et al.* (1996), one can show that for the most interesting and physically relevant case of $\sigma = 2$, the *condition of soliton stability* is given by the simple formula

$$\frac{\partial \tilde{Q}}{\partial \beta} > 0\,, \tag{9}$$

where $\tilde{Q} \equiv Q(\beta - C_x^2/4 - C_y^2/4, 0, 0)$, which means that one has to calculate the invariant (energy) on a fundamental family of radially symmetric stationary soliton solutions $\{V_s(\beta - C_x^2/4 - C_y^2/4, 0, 0; x, y), W_s(\beta - C_x^2/4 - C_y^2/4, 0, 0; x, y)\}$. Analysis of the behaviour of the power invariant $\tilde{Q}$ (verified by direct numerical simulations) shows that the unstable $\chi^{(2)}$ spatial solitons can only exist for $\Delta < 0$, whereas for $\Delta \geq 0$ all solitons are stable. This result holds both for (2+1)-dimensional (Buryak *et al.* 1995) and (1+1)-dimensional (Pelinovsky *et al.* 1995) cases.

3. Different Regimes of Soliton Interactions

Using the methods of Gorshkov and Ostrovsky (1981), we can derive a general system of ordinary differential equations (ODEs) for the soliton parameters, describing the adiabatic interaction of two almost identical solitons in a bulk $\chi^{(2)}$ medium. This is based on two major assumptions: (i) that the relative distance R between solitons is large ($R \gg 1$, the approximation of well-separated solitons), and (ii) the relative soliton velocity C is small ($C \ll 1$). Below we give an outline of the derivation procedure, omitting the technical details which can be found in Buryak and Steblina (1999).

We take two well-separated one-soliton solutions of equations (3) as the zeroth approximation of a nonstationary two-soliton solution. Then we allow all internal parameters of both solitons to depend on a *slow* variable Z (where $Z \equiv \varepsilon z$) and look for an asymptotic two-soliton solution of equations (3) in the form of infinite series, with ε being a small parameter of the asymptotic procedure. This approach is self-consistent only if certain compatibility conditions are satisfied. These compatibility conditions lead to a system of ODEs that is a lot simpler than the original model (3), but is still too complex to provide immediate physical insight. However, this system can be simplified further using additional assumptions.

Let us consider *two initially identical solitons*, which are located symmetrically about the coordinate centre $(0,0)$ in the (x,y) plane, and have opposite initial velocities. In other words, initially $C_x^{(1)} = -C_x^{(2)}$, $C_y^{(1)} = -C_y^{(2)}$, with superscripts (1) and (2) referring to first and second solitons respectively. Using these assumptions we can obtain the following analytic system for adiabatically changing soliton parameters:

$$
\begin{aligned}
&-\frac{\partial \tilde{Q}^{(1)}}{\partial \beta^{(1)}}\ddot{\phi}^{(1)} + \tfrac{1}{2}\frac{\partial U}{\partial \phi^{(1)}} = 0,\\
&-\frac{\partial \tilde{Q}^{(2)}}{\partial \beta^{(2)}}\ddot{\phi}^{(2)} + \tfrac{1}{2}\frac{\partial U}{\partial \phi^{(2)}} = 0,\\
&\frac{\tilde{Q}^{(1)}}{2}\ddot{x}^{(1)} + \tfrac{1}{2}\frac{\partial U}{\partial x^{(1)}} = 0,\\
&\frac{\tilde{Q}^{(2)}}{2}\ddot{x}^{(2)} + \tfrac{1}{2}\frac{\partial U}{\partial x^{(2)}} = 0,\\
&\frac{\tilde{Q}^{(1)}}{2}\ddot{y}^{(1)} + \tfrac{1}{2}\frac{\partial U}{\partial y^{(1)}} = 0,\\
&\frac{\tilde{Q}^{(2)}}{2}\ddot{y}^{(2)} + \tfrac{1}{2}\frac{\partial U}{\partial y^{(2)}} = 0,
\end{aligned}
\tag{10}
$$

where $\phi^{(j)}(z)$, $x^{(j)}(z)$ and $y^{(j)}(z)$ denote soliton phases and centre positions, and the potential U can be written in terms of soliton overlap integrals. The exact definition of the potential U will be given below.

(3a) Effective Particle Approach

System (10) has the form of the classical mechanics problem for two particles interacting in three-dimensional space. However, each of these effective particles has a variable anisotropic mass, and $M_\phi^{(j)} \neq M_x^{(j)} = M_y^{(j)}$. In addition, $M_\phi^{(j)} \equiv -2\partial\tilde{Q}^{(j)}/\partial\beta^{(j)}$ is always *negative*, because the stability condition (9) for single solitons requires $\partial\tilde{Q}^{(j)}/\partial\beta^{(j)} > 0$.

We now multiply the first of equations (10) by $\partial\tilde{Q}^{(2)}/\partial\beta^{(2)}$ the second by $\partial\tilde{Q}^{(1)}/\partial\beta^{(1)}$, and subtract the resulting equations from each other. Applying a similar procedure to the other two pairs of equations in the system (10), we obtain

$$M_\phi\ddot{\phi} + \frac{\partial U}{\partial\phi} = 0,$$

$$M_X\ddot{X} + \frac{\partial U}{\partial X} = 0, \tag{11}$$

$$M_Y\ddot{Y} + \frac{\partial U}{\partial Y} = 0,$$

where $M_\phi \equiv -2Q^{(1)}_{\beta^{(1)}}Q^{(2)}_{\beta^{(2)}}/(Q^{(1)}_{\beta^{(1)}} + Q^{(2)}_{\beta^{(2)}})$, $Q^{(j)}_{\beta^{(j)}} \equiv \partial Q^{(j)}/\partial\beta^{(j)}$, $M_X = M_Y \equiv Q^{(1)}Q^{(2)}/(Q^{(1)} + Q^{(2)})$, $\phi \equiv \phi^{(2)} - \phi^{(1)}$, $X \equiv x^{(2)} - x^{(1)}$ and $Y \equiv y^{(2)} - y^{(1)}$, i.e. ϕ is the relative phase between the solitons, X and Y being the separations between solitons in the x and y directions respectively.

The reduction of equations (10) to (11) is self-consistent if M_ϕ, M_X, and M_Y depend only on $\Delta\beta \equiv \beta^{(2)} - \beta^{(1)}$ or are constants. In this subsection we assume all effective masses to be constants, i.e. $M_\phi = M_\phi(\beta_0)$, $M_X = M_X(\beta_0)$ and $M_Y = M_Y(\beta_0)$, where $\beta_0 \equiv \beta^{(1)}(z=0) = \beta^{(2)}(z=0)$, prohibiting power exchange between the solitons. Violation of this assumption and soliton power exchange are addressed in the next subsection.

Following the standard methods of classical mechanics (see e.g. Goldstein 1980), the dimensionality of equation (11) can be reduced using cylindrical coordinates (R, ϕ), where $R \equiv \sqrt{X^2 + Y^2}$ is the relative distance between the interacting beams. The final equations can then be presented in the form

$$M_\phi\ddot{\phi} + \frac{\partial U_{\text{eff}}}{\partial\phi} = 0; \quad M_R\ddot{R} + \frac{\partial U_{\text{eff}}}{\partial R} = 0\,, \tag{12}$$

which corresponds to the effective two-dimensional Lagrangian

$$L = \tfrac{1}{2}M_R\,\dot{R}^2 + \tfrac{1}{2}M_\phi\,\dot{\phi}^2 - U_{\text{eff}}(R,\phi)\,. \tag{13}$$

The elements of the effective mass matrix for the case of two identical solitons are defined as

$$M_R \equiv \pi\int_0^\infty \{|V_s(r)|^2 + 2\sigma|W_s(r)|^2\}r\,dr,$$

$$M_\phi \equiv -2\partial M_R/\partial\beta\,, \tag{14}$$

where the integrand is calculated for the fundamental one-soliton stationary solutions of radial symmetry that are involved in the interaction. The effective potential energy has the form

$$U_{\mathrm{eff}}(R,\phi) = \frac{M_R S^2 C_0^2}{2R^2} + U_1(R)\cos(\phi) + U_2(R)\cos(2\phi)\,, \tag{15}$$

where the overlap integrals U_1 and U_2 are given by

$$U_1(R) \equiv -2\int_{-\infty}^{\infty}\int_{-\infty}^{\infty}\left[W_s^{(2)}V_s^{(2)}V_s^{(1)} + W_s^{(1)}V_s^{(1)}V_s^{(2)}\right]dx\,dy,$$

$$U_2(R) \equiv -\int_{-\infty}^{\infty}\int_{-\infty}^{\infty}\left[{V_s^{(2)}}^2 W_s^{(1)} + {V_s^{(1)}}^2 W_s^{(2)}\right]dx\,dy,$$

where $V_s^{(1)} = V_s(\beta,0,0;x-R/2,y)$, $W_s^{(1)} = W_s(\beta,0,0;x-R/2,y)$, $V_s^{(2)} = V_s(\beta,0,0;x+R/2,y)$ and $W_s^{(2)} = W_s(\beta,0,0;x+R/2,y)$. The impact parameter S defines the distance between the trajectories of non-interacting solitons, and $C_0 \equiv \dot{R}(z=0)$ is the relative velocity between the solitons prior to the interaction.

When the distance between the interacting solitons is relatively large, the soliton interaction is determined by their tail asymptotics, which can be found analytically (except for constant factors A and B) as $V^{(j)}(r) = (A/\sqrt{r})\exp(-\sqrt{\beta}r)$, $W^{(j)}(r) = (B/\sqrt{r})\exp[-\sqrt{\sigma(2\beta+\Delta)}r]$ for $\sigma(2\beta+\Delta) \le 4\beta$, and $W^{(j)}(r) = A^2/\{r[\sigma(2\beta+\Delta)-4\beta]\}\exp(-2\sqrt{\beta}r)$ for $\sigma(2\beta+\Delta) > 4\beta$. The asymptotic expressions for the functions U_1 and U_2 can be also estimated analytically, e.g.

$$U_1(R) \approx -K_1 A^2(\beta)^{1/4}\exp(-\sqrt{\beta}R)/\sqrt{R}\,, \tag{16}$$

where the positive parameter K_1 is fitted numerically. We found that for a large range of parameters Δ and β, $K_1 = 20{\cdot}8 \pm 0{\cdot}2$. The situation with $U_2(R)$ is more complicated. For $\sqrt{\sigma(\Delta+2\beta)} < 2\sqrt{\beta}$ (i.e. $\Delta < 0$ for $\sigma = 2$), the potential $U_2(R) \sim \exp[-\sqrt{\sigma(\Delta+2\beta)}R]$, whereas for $\sqrt{\sigma(\Delta+2\beta)} \ge 2\sqrt{\beta}$ (i.e. $\Delta \ge 0$ for $\sigma = 2$), the potential $U_2(R) \sim \exp[-2\sqrt{\beta}R]$. In both cases further numerical fitting is necessary. We found that for the $\Delta < 0$, $\sigma = 2$ case,

$$U_2(R) \approx -K_2 B^2[2(\Delta+2\beta)]^{1/4}\exp[-\sqrt{2(\Delta+2\beta)}R]/\sqrt{R}\,, \tag{17}$$

where again the positive parameter K_2 is fitted numerically to be $K_2 = 20{\cdot}0 \pm 1{\cdot}0$, although the accuracy of this approximation is clearly worse than that for equation (16). For the $\Delta \ge 0$, $\sigma = 2$ case, $U_2(R) \ll U_1(R)$ and usually can be ignored.

However, for the combination of parameter values discussed in this paper ($\Delta = 1$, $\beta = 0\cdot 5$), we still adopted the following fitting formulas for both $U_1(R)$ and $U_2(R)$:

$$
\begin{aligned}
U_1(R) &= -2330\cdot 0 \exp(-0\cdot 7071\, R)/\sqrt{R}, \\
U_2(R) &= -8216\cdot 0 \exp(-1\cdot 4142\, R)\,,
\end{aligned}
\tag{18}
$$

which are a good approximation for $R > 5\cdot 0$.

The effective mechanical model defined by the Lagrangian (13) can be used to generate a physical picture of soliton dynamics predicting the outcome of soliton collisions. Importantly, interaction forces depend strongly on the relative phase ϕ. For simplicity, we first consider the case when $U_2 \ll U_1$ (which is always true for $\Delta > 0$) and $\phi = 0, \pi$. In the case of out-of-phase collisions ($\phi = \pi$), the 'centrifugal force' defined by the first term of the effective potential $U_{\rm eff}$, and the direct interaction force defined by the second term $U_1(R)\cos(\phi)$, are both *repulsive*. Therefore the effective particle cannot reach the force centre, i.e. solitons cannot fuse (see Fig. 3*a*). The interaction scenario is very different for in-phase soliton collisions ($\phi = 0$). An interplay between a repulsive 'centrifugal' force and an attractive interaction force leads to two qualitatively different regimes shown schematically in Fig. 3*b*. For low relative velocities (and/or sufficiently large values of the impact parameter S), solitons cannot overcome the centrifugal potential barrier, and they spiral about each other. At higher velocities (and/or smaller values of the impact parameter S) solitons can closely approach each other and fusion may occur.

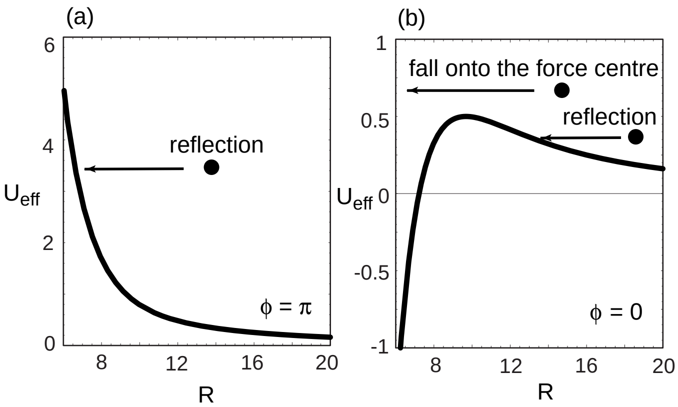

Fig. 3. Qualitative sketch of the effective interaction potential $U_{\rm eff}(R,\phi)$ for (*a*) the out-of-phase interaction ($\phi = \pi$) and (*b*) the in-phase interaction ($\phi = 0$).

The numerical analysis of this paper is based on the standard split-step beam propagation method (see e.g. Taha and Ablowitz 1984), where we use a 256×256 grid with periodic boundary conditions and step size $\Delta z = 0\cdot 005$. Our direct numerical modelling of equations (3) confirms the predictions of the approximate model given by the Lagrangian (13). Figs 4*a*–4*c* present characteristic examples

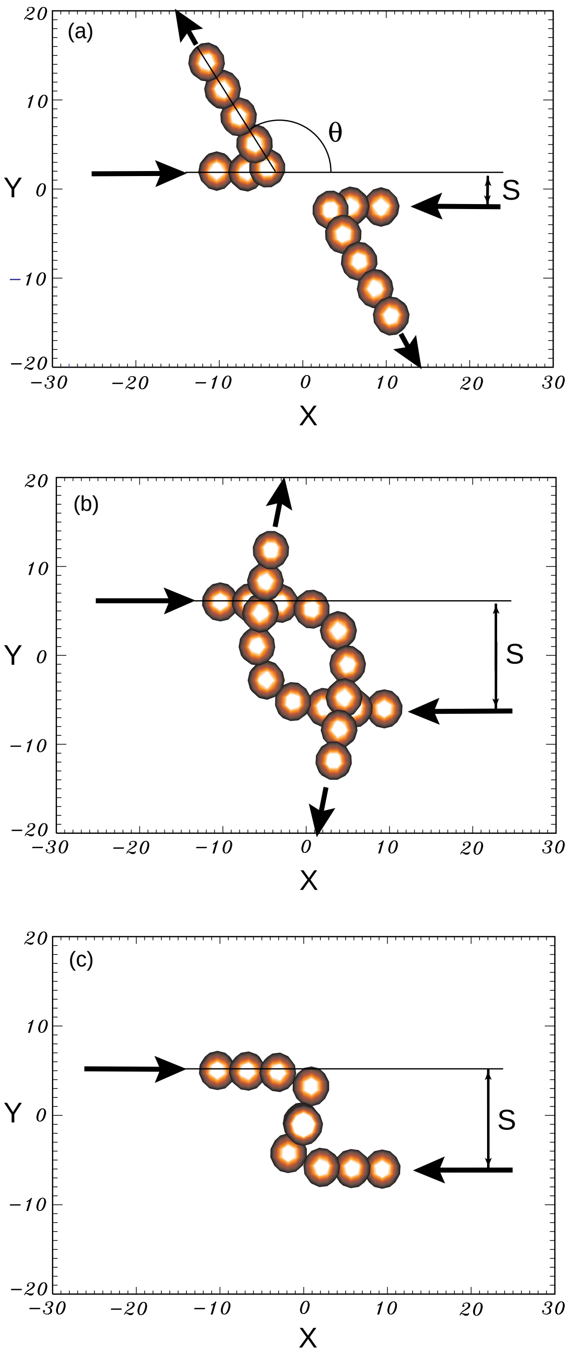

Fig. 4. Sequences of soliton positions in the (X,Y) plane shown at different propagation distances for (a) soliton scattering ($\phi = \pi$, $S = 3{\cdot}6$), (b) soliton reflection via spiralling ($\phi = 0$, $S = 11{\cdot}6$), and (c) soliton fusion ($\phi = 0$, $S = 11{\cdot}0$). All results are obtained for $\beta = 0{\cdot}5$, $\Delta = 1{\cdot}0$ and $C_0 = 0{\cdot}2$. Here and in subsequent figures only the positions of the first harmonic components are shown (the second harmonic components always closely follow the corresponding first harmonic components).

of the soliton interaction, including soliton scattering (4a), soliton spiralling (4b), and soliton fusion (4c). The corresponding three-dimensional views of soliton spiralling and soliton fusion are shown in Fig. 5. All of the types of soliton interaction predicted by the analytical model have been observed in the numerics. To make a quantitative comparison, we integrated the dynamical model for the relative coordinate and phase following from equation (13), applying the techniques of the well-known scattering theory of classical mechanics (Goldstein 1980). Fig. 6 compares the results of our analytical model with those of a direct numerical experiment, showing the dependence of the scattering angle θ on the soliton impact parameter S. Good agreement is found even for the case of initial relative velocity $C_0 = 0{\cdot}2$.

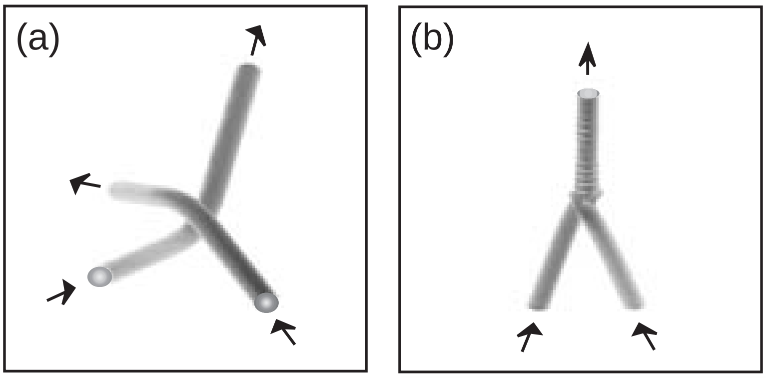

Fig. 5. Three-dimensional view of soliton interactions. In (a) the parameters are the same as in Fig. 4b; in (b) they are the same as in Fig. 4c).

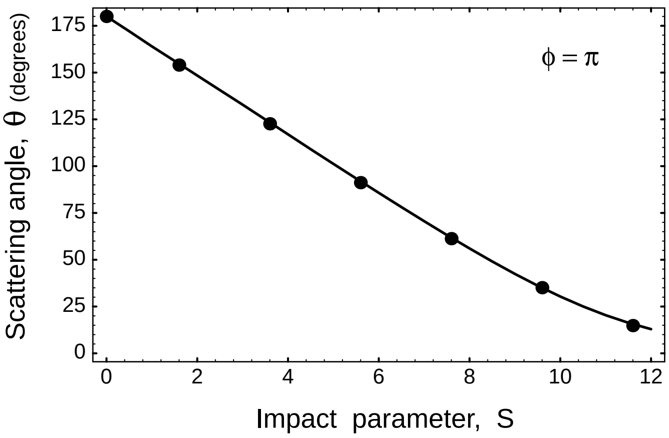

Fig. 6. Soliton scattering angle θ versus impact parameter S (see definitions in Fig. 4a) for out-of-phase collisions ($\phi = \pi$). Solid line: analytical results; dots: results of numerical simulations. Results are obtained for $\beta = 0{\cdot}5$, $\Delta = 1{\cdot}0$, and $C_0 = 0{\cdot}2$.

(3b) Power Exchange between Colliding Solitons

To describe the power exchange between the interacting solitons, we approximate $Q^{(1)}$ and $Q^{(2)}$ as linear functions of $\beta^{(1)}$ and $\beta^{(2)}$, respectively. This leads to the following dependences of $Q^{(1)}$ and $Q^{(2)}$ on $\Delta\beta$ $[\Delta\beta \equiv \beta^{(2)} - \beta^{(1)}]$:

$$Q^{(1)} = Q - \tfrac{1}{2}\frac{\partial Q}{\partial \beta_0}\Delta\beta; \quad Q^{(2)} = Q + \tfrac{1}{2}\frac{\partial Q}{\partial \beta_0}\Delta\beta\,, \tag{19}$$

where $\partial Q/\partial\beta_0 \equiv \partial Q/\partial\beta|_{\beta=\beta_0}$, $\beta \equiv (\beta^{(2)} + \beta^{(1)})/2$ and $Q \equiv Q^{(1)}(\beta_0) = Q^{(2)}(\beta_0)$. Equations (19) are consistent with total energy conservation: $Q^{(1)} + Q^{(2)} = 2Q =$ const. Using (19), we find that

$$\begin{aligned} M_\phi &= \, - Q_{\beta_0} = \text{const}, \\ M_X &= M_Y = Q/2 - Q_{\beta_0}^2(\Delta\beta)^2/8\,. \end{aligned} \tag{20}$$

Thus for small changes of relative phase ϕ (implying that $\Delta\beta = \dot\phi$ is also small), all of the masses M_ϕ, M_X and M_Y are constants, correct to order $(\Delta\beta)^2$. These qualitative arguments show why we can assume the masses to be constants in equations (11).

We can calculate the small power exchange between harmonics by simply integrating equations (12), and measuring $\Delta\beta = \dot\phi$ at some z sufficiently far after the collision region. In general, after the interaction we have $\Delta\beta \neq 0$ for any soliton collision with initial $\phi_0 \neq 0, \pi$. The exchanged power is then given by

$$\Delta Q = \frac{\partial Q}{\partial \beta_0}\Delta\beta\,, \tag{21}$$

where $\partial Q/\partial\beta_0$ is calculated for either of the two identical solitons prior to their interaction. Fig. 7 gives an example of soliton collision with significant power exchange.

It is evident from Fig. 7 that, after the collision, the relative soliton velocity has increased. This can be readily explained using dynamical invariants of equations (12). Consider the total energy of the two particles approaching each other from a sufficiently large distance:

$$H_{\text{in}} = \tfrac{1}{2}M_R\,\dot R^2 + \tfrac{1}{2}M_\phi\,\dot\phi^2\,. \tag{22}$$

In equation (22) we have neglected the potential energy of interaction, $U_{\text{eff}}(R,\phi)$. The total energy H_{out} long after the interaction has the same form as H_{in} and must retain the same value as before the interaction. Accordingly, since $\dot\phi^2 > 0$ and $M_\phi < 0$, the growth of $\dot\phi$ has to be compensated for by the growth of relative velocity $\dot R$. This explains the widening of scattering angles after soliton interaction which has been observed in our numerical simulations (e.g. Fig. 7) and by others (e.g. Snyder *et al*. 1998), and provides us with a potentially important tool for soliton acceleration.

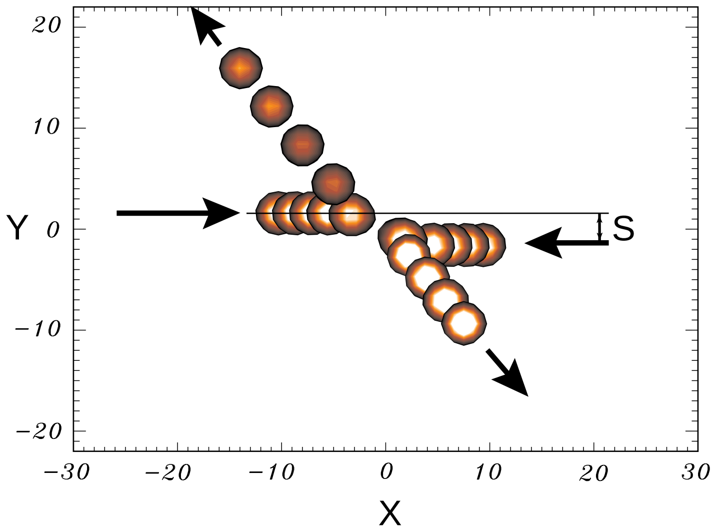

Fig. 7. Sequences of soliton positions in the (X,Y) plane, shown at different propagation distances for soliton scattering ($\phi = \pi/8$, $S = 3{\cdot}2$) with significant power exchange. Results are obtained for $\beta = 0{\cdot}5$, $\Delta = 1{\cdot}0$, and $C_0 = 0{\cdot}2$.

To verify our theoretical predictions we compare the power exchange results given by equation (21) with the results of direct numerical modelling. Fig. 8 demonstrates that equation (21) can give approximately correct results even when significant soliton power exchange occurs, and the condition $\Delta\beta \ll 1$ is violated.

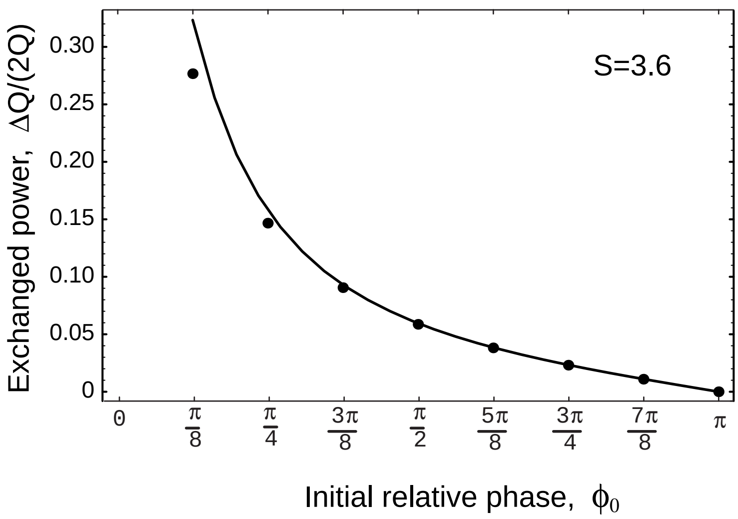

Fig. 8. Normalised exchanged power between the solitons $\Delta Q/2Q$ versus initial relative phase ϕ_0. Solid line: analytical results, dots: results of numerical simulations. Results are obtained for $S = 3{\cdot}6$, $\beta = 0{\cdot}5$, $\Delta = 1{\cdot}0$, and $C_0 = 0{\cdot}2$.

(3c) Stability of Spiralling Configurations

Using the analytical model, we can investigate the possibility of stable spiralling configurations (or bound states) similar to those observed for incoherently interacting photorefractive solitons (Shih *et al*. 1997; Buryak *et al*. 1999). For two (2+1)-dimensional $\chi^{(2)}$ solitons interacting coherently with a positive phase mismatch and $U_1 \gg U_2$, the model (13) predicts the existence of a local minimum in R of the effective interaction potential $U_{\rm eff}(R)$ at $\phi = 0$ and $R_0 \sim 1$. However, the approximate model (13) is valid only for weakly overlapping solitons when R is large and, therefore, this minimum is physically unrealisable, being located in the region of soliton fusion. In the opposite situation of negative phase matching, U_1 and U_2 may become comparable, and in a certain range of parameters we find a shallow local minimum of the potential $U_{\rm eff}(R)$ at $\phi = \pi$ and $R_0 \gg 1$. A spiralling configuration of two solitons, corresponding to such a local minimum, would be stable if both mass coefficients (masses) were positive. Unfortunately, stability of the single solitons involved in the interaction always requires that $M_\phi < 0$ [see the condition (9)], and therefore this extremum is a *saddle point* in the space (R, ϕ), implying the instability of the corresponding bound states. Indeed, we have not been able to observe such states in extensive direct numerical modelling of equations (3). We expect this to be a rather general phenomenon, valid for other types of solitary waves interacting coherently, which, however, has not been previously addressed in the literature.

4. Physical Estimates

In order to provide parameter values for the experimental observation of $\chi^{(2)}$ soliton collisions, we need to estimate two key parameters, the minimum intensity required for soliton formation and the minimum interaction length necessary for the observation of switching.

An expression estimating the minimum intensity has recently been obtained (Buryak *et al*. 1997), and is given by

$$I_{\rm min} = \frac{G k_1}{\omega_1^5 [\chi^{(2)}]^2 R_0^4}\,, \tag{23}$$

where R_0 is the soliton width [defined in Buryak *et al*. (1997) as full width at half maximum for E_2 harmonic amplitude], $\chi^{(2)}$ is the effective quadratic coefficient, k_1 and ω_1 are the wave-number and frequency, respectively, for the fundamental harmonic, and G is a constant that does not depend on the material or the experimental setup parameters. For example, let us take typical values for type II SHG in KTP, similar to the ones reported by Torruellas *et al*. (1995): $R_0 = 10\,\mu$m, $\omega_1/c = 6{\cdot}13 \times 10^4\,{\rm cm}^{-1}$, $k_1 = 10{\cdot}5\,\mu{\rm m}^{-1}$ and $\chi^{(2)} = 6\,{\rm pm\,V}^{-1}$. Using the formalism of Buryak *et al*. (1997), we obtain $I_{\rm min} \approx 14{\cdot}0\,{\rm GW\,cm}^{-2}$ for (2+1)-dimensional solitons.

Our numerical results indicate that the minimum interaction length $L_{\rm min}$ necessary for switching is about 10 normalised propagation distance units, i.e. of the order of 10 diffraction lengths. Again, taking the experimental parameters as $R_0 = 10\,\mu$m and $k_1 = 10{\cdot}5\,\mu{\rm m}^{-1}$, we can calculate that $R_{\rm d} \approx 2\,$mm. Thus the minimum necessary crystal length in physical units is $L_{\rm min} = 10 R_{\rm d} \approx 2\,$cm.

We point out that our values of $I_{\min}$ and $L_{\min}$ give an estimate from below. Our calculations are based on the assumption that the laser beams initially match exactly each of the corresponding soliton components. Breaking this condition, e.g. by generating $\chi^{(2)}$ solitons without seeding of the second harmonic, should slightly increase the required threshold intensity and interaction length. On the other hand, the use of new materials and/or phase-matching techniques can lead to much higher values of the effective $\chi^{(2)}$ parameter which, in turn, significantly decreases $I_{\min}$, or (if R_0 is decreased) $L_{\min}$. For example, the use of the so-called quasi-phase-matching (QPM) technique (see e.g. Fejer *et al*. 1992; Miller *et al*. 1997) can increase the value of the effective $\chi^{(2)}$ parameter for conventional nonlinear crystals by up to $50\,\mathrm{pm\,V^{-1}}$, thus lowering the required laser intensity to $I_{\min} \sim 100\,\mathrm{MW\,cm^{-2}}$. The use of semiconductor optical materials (plus quantum-well-based QPM) can lead to even higher effective $\chi^{(2)}$ nonlinearities (Ueno *et al*. 1997), thus reducing the required $I_{\min}$ further, potentially allowing soliton-based all-optical switching to be achieved at the intensity level of just a few MW cm^{-2}.

5. Conclusions

In this paper we have analysed non-planar collisions of (2+1)-dimensional $\chi^{(2)}$ solitons and demonstrated a controllable soliton-based all-optical switching determined by the initial soliton states, i.e. the soliton velocities, the relative phase, and the impact parameter. We have derived an effective mechanical model that provides a physical description of soliton collisions in terms of an effective particle in a central force. This model has been fully confirmed by the results of direct numerical simulations. The phenomena of $\chi^{(2)}$ soliton scattering and power exchange may find applications in ultra-fast all-optical signal processing and switching in a bulk medium. Our approach can be readily generalised for the analysis of interactions of higher-dimensional solitons (including the so-called 'light bullets'; Malomed *et al*. 1997) in $\chi^{(2)}$ materials and other types of nonlinear media.

Acknowledgments

The authors are grateful to Yu. S. Kivshar, B. A. Malomed and M. Segev for useful discussions and suggestions. Both authors acknowledge support from the Australian Research Council.

References

Azimov, B. S., Sukhorukov, A. P., and Truhov, D. V. (1987). *Bull. Russ. Acad. Sci. (Phys.)* **51**, 19.
Baek, Y., Schiek, R., and Stegeman, G. I. (1995). *Opt. Lett.* **20**, 2168.
Baek, Y., Schiek, R., Stegeman, G. I., Baumann, I., and Sohler, W. (1997). *Opt. Lett.* **22**, 1550.
Buryak, A. V., and Kivshar, Yu. S. (1995). *Phys. Lett.* A **197**, 407.
Buryak, A. V., and Steblina, V. V. (1999). *J. Opt. Soc. Am.* B **16**, 245.
Buryak, A. V., Kivshar, Yu. S., and Steblina, V. V. (1995). *Phys. Rev.* A **52**, 1670.
Buryak, A. V., Kivshar, Yu. S., and Trillo, S. (1996). *Phys. Rev. Lett.* **77**, 5210.
Buryak, A. V., Kivshar, Yu. S., and Trillo, S. (1997). *J. Opt. Soc. Am.* B **14**, 3110.
Buryak, A. V., Kivshar, Yu. S., Shih, M., and Segev, M. (1999). *Phys. Rev. Lett.* **82**, 81.
Costantini, B., De Angelis, C., Barthelemy, A., Bourliaguet, B., and Kermene, V. (1998). *Opt. Lett.* **23**, 424.

De Salvo, R., Hagan, D. J., Sheik-Bahae, M., Stegeman, G. I., and Van Stryland, E. W. (1992). *Opt. Lett.* **17**, 28.
Duree, G. C., Shultz, J. L., Salamo, G. J., Segev, M., Yariv, A., Crosignani, B., Di Porto, P., Sharp, E. J., and Neurgaonkar, R. R. (1993). *Phys. Rev. Lett.* **71**, 553.
Etrich, C., Peschel, U., Lederer, F., Malomed, B., and Kivshar, Yu. S. (1996). *Phys. Rev.* E **54**, 4321.
Fejer, M. M., Magel, G. A., Jundt, D. H., and Byer, R. L. (1992). *IEEE J. Quant. Electron.* **28**, 2631.
Friberg, S. R., Weiner, A. M., Silberberg, Y., Sfez, B. G., and Smith, P. S. (1988). *Opt. Lett.* **13**, 904.
Goldstein, H. (1980). 'Classical Mechanics', Chap. 3 (Addison–Wesley: Reading, Mass.).
Gorshkov, K. A., and Ostrovsky, L. A. (1981). *Physica* D **3**, 428.
Jensen, S. M. (1982). *IEEE J. Quant. Electron.* **QE-18**, 1580.
Karpman, V. I., and Solov'ev, V. V. (1981). *Physica* D **3**, 487.
Kawachi, M. (1990). *Opt. Quant. Electron.* **22**, 391.
Leo, G., Assanto, G., and Torruellas, W. E. (1997*a*). *Opt. Commun.* **134**, 223.
Leo, G., Assanto, G., and Torruellas, W. E. (1997*b*). *Opt. Lett.* **22**, 7.
Malomed, B., Drummond, P., He, H., Berntson, A., Anderson, D., and Lisak, M. (1997). *Phys. Rev.* E **56**, 4725.
Menyuk, C. R., Schiek, R., and Torner, L. (1994). *J. Opt. Soc. Am.* B **11**, 2434.
Miller, G. D., Batchko, R. G., Tulloch, W. M., Weise, D. R., Fejer, M. M., and Byer, R. L. (1997). *Opt. Lett.* **22**, 1834.
Miller, S. E. (1969). *Bell Syst. Tech. J.* **48**, 2059.
Pelinovsky, D. E., Buryak, A. V., and Kivshar, Yu. S. (1995). *Phys. Rev. Lett.* **75**, 591.
Schubert, M., and Wilhelmi, B. (1986). 'Nonlinear Optics and Quantum Electronics' (Wiley: New York).
Segev, M., and Stegeman, G. I. (1998). *Phys. Today* **51**, 42 and references therein.
Shen, T. P., Stegeman, G. I., and Maradudin, A. A. (1988). *Appl. Phys. Lett.* **52**, 1.
Shih, M., Segev, M., and Salamo, G. (1997). *Phys. Rev. Lett.* **78**, 2551.
Snyder, A. W., and Love, J. D. (1983). 'Optical Waveguide Theory' (Chapman and Hall: London).
Snyder, A. W., Buryak, A. V., and Mitchell, D. J. (1998). *Opt. Lett.* **23**, 4.
Steblina, V. V., Kivshar, Yu. S., Lisak, M., and Malomed, B. A. (1995). *Opt. Commun.* **118**, 345.
Steblina, V. V., Kivshar, Yu. S., and Buryak, A. V. (1998). *Opt. Lett.* **23**, 156.
Stegeman, G. I., Wright, E. M., Finlayson, N., Zanoni, R., and Seaton, C. T. (1988). *J. Lightwave Technol.* **6**, 953.
Stegeman, G. I., Hagan, D. J., and Torner, L. (1996). *J. Opt. Quant. Electron.* **28**, 1691.
Taha, T. P., and Ablowitz, M. J. (1984). *J. Comp. Phys.* **55**, 203.
Tikhonenko, V., Christou, J., and Luther-Davies, B. (1995). *J. Opt. Soc. Am.* B **12**, 2046.
Torruellas, W. E., Wang, Z., Hagan, D. J., Van Stryland, E. W., Stegeman, G. I., Torner, L., and Menyuk, C. R. (1995). *Phys. Rev. Lett.* **74**, 5036.
Ueno, Y., Stegeman, G. I., and Tajima, K. (1997). *Jpn J. Appl. Phys.* **36**, L613.
Wa, P. Li Kam, Robson, P. N., Roberts, J. S., Pate, M. A., and David, J. P. R. (1988). *Appl. Phys. Lett.* **52**, 2013.

Manuscript received 23 December 1998, accepted 6 April 1999